Report

Cell Reports

Rad5 Plays a Major Role in the Cellular Response to DNA Damage during Chromosome Replication

Graphical Abstract

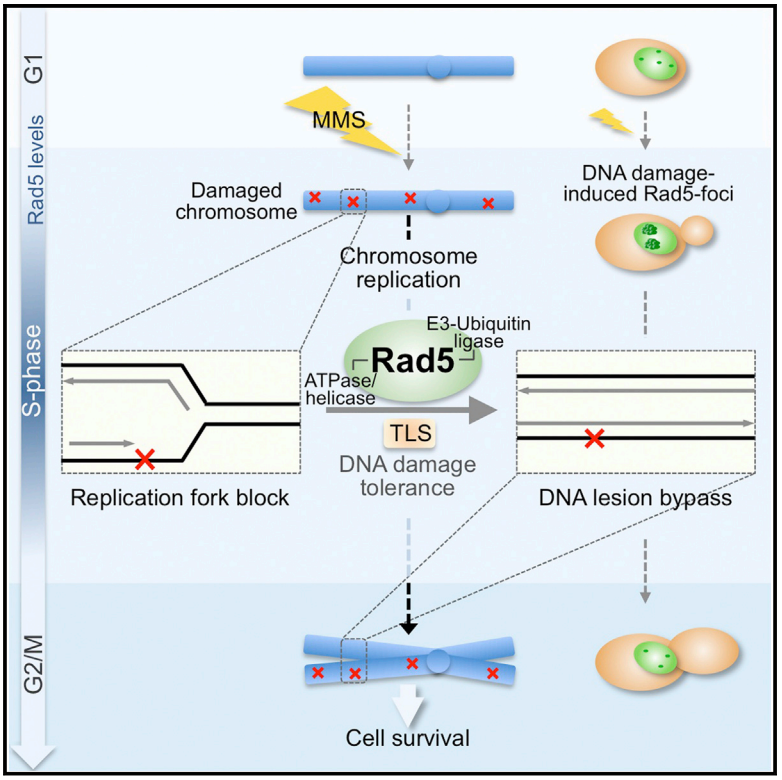

Highlights

MMS-induced DNA lesions are mainly tolerated by the error-free Rad5 pathway

Rad5 is required for replication fork progression through MMS-damaged DNA

Rad5 Ub-ligase and ATPase/helicase activities are required for the response to MMS

Rad5 peaks during S phase and forms subnuclear foci in response to DNA damage

Authors

María Ángeles Ortiz-Bazán, María Gallo--Fernández, ..., María Victoria Vázquez, José Antonio Tercero

Correspondence

jatercero@cbm.csic.es

In Brief

Ortiz-Bazán et al. now show that tolerance to methyl methanesulfonate (MMS)-induced DNA lesions during S phase is carried out mainly by Rad5-mediated, error-free damage bypass. Rad5 allows the progression of replication forks through MMS-damaged DNA, ensuring the completion of chromosome replication while minimizing mutagenesis, all of which are crucial for genome stability.

Ortiz-Bazán et al., 2014, Cell Reports 9, 460–468
October 23, 2014 ©2014 The Authors
http://dx.doi.org/10.1016/j.celrep.2014.09.005

OPEN ACCESS
CellPress

Cell Reports
Report

Rad5 Plays a Major Role in the Cellular Response to DNA Damage during Chromosome Replication

María Ángeles Ortiz-Bazán,[1] María Gallo-Fernández,[1] Irene Saugar,[1] Alberto Jiménez-Martín,[1] María Victoria Vázquez,[1] and José Antonio Tercero[1,*]
[1]Centro de Biología Molecular Severo Ochoa (CSIC/UAM), Cantoblanco, 28049 Madrid, Spain
*Correspondence: jatercero@cbm.csic.es
http://dx.doi.org/10.1016/j.celrep.2014.09.005

SUMMARY

The *RAD6/RAD18* pathway of DNA damage tolerance overcomes unrepaired lesions that block replication forks. It is subdivided into two branches: translesion DNA synthesis, which is frequently error prone, and the error-free DNA-damage-avoidance subpathway. Here, we show that Rad5$^{HLTF/SHPRH}$, which mediates the error-free branch, has a major role in the response to DNA damage caused by methyl methanesulfonate (MMS) during chromosome replication, whereas translesion synthesis polymerases make only a minor contribution. Both the ubiquitin-ligase and the ATPase/helicase activities of Rad5 are necessary for this cellular response. We show that Rad5 is required for the progression of replication forks through MMS-damaged DNA. Moreover, supporting its role during replication, this protein reaches maximum levels during S phase and forms subnuclear foci when replication occurs in the presence of DNA damage. Thus, Rad5 ensures the completion of chromosome replication under DNA-damaging conditions while minimizing the risk of mutagenesis, thereby contributing significantly to genome integrity maintenance.

INTRODUCTION

The conserved *RAD6/RAD18* pathway of DNA damage tolerance (DDT) plays a crucial role in genome stability, allowing the bypass of unrepaired DNA lesions that hamper replication forks (Branzei, 2011; Chang and Cimprich, 2009; Saugar et al., 2014; Ulrich, 2011). This pathway can be subdivided into two branches: translesion DNA synthesis (TLS) and the damage-avoidance subpathway. TLS uses specialized, low-fidelity DNA polymerases that can replicate directly across the lesions in a frequently mutagenic process (Sale, 2013). In contrast, the damage-avoidance branch mediates damage bypass by transient template switching, in which the blocked DNA nascent strand uses the newly synthesized, undamaged strand of the sister chromatid as a template for replication over the DNA lesion, in a process that is error free (Branzei, 2011; Ulrich, 2011). In budding yeast, damage avoidance is mediated by the E3-ubiquitin ligase Rad5 (HLTF and SHPRH in humans), a protein that also has ATPase activity, together with the E2-conjugating complex Mms2-Ubc13^{UEV1} (Unk et al., 2010). DDT mechanisms are controlled by posttranslational modifications of proliferating cell nuclear antigen (PCNA), the processivity factor for DNA polymerases (Branzei, 2011; Chang and Cimprich, 2009; Saugar et al., 2014; Ulrich, 2011). Thus, in response to many types of DNA damage or replicative stress, PCNA is monoubiquitylated by Rad6/Rad18, leading to the recruitment of TLS polymerases. PCNA can be further polyubiquitylated by Rad5$^{HLTF/SHPRH}$-Mms2-Ubc13^{UEV1}, triggering the damage-avoidance subpathway.

Although the two branches of the *RAD6/RAD18* pathway adopt distinct strategies for damage bypass, one might expect that to avoid mutagenesis, the error-free subpathway would be generally favored. However, this preference is not obvious, and little is known about how cells choose between TLS and template switching. This choice appears to depend on the nature of the DNA lesions as well as on the extent of the damage or the timing of the cellular response. For example, in human cells, DNA lesions induced by UV light or tobacco smoke are preferentially bypassed by TLS (Izhar et al., 2013). In budding yeast, DNA lesions induced by acute exposure to UV light are mainly bypassed by TLS (Daigaku et al., 2010), but damage avoidance is more important during chronic low-dose UV exposure (Hishida et al., 2009). Likewise, either branch of *RAD6/RAD18* is sufficient for cell survival after treatment with a low dose of methyl methanesulfonate (MMS), but the preferential use of one over the other is cell-cycle dependent (Huang et al., 2013). Interestingly, DNA bending facilitates template switching, revealing that chromatin architecture is also a fundamental factor that influences the mode of DDT (Gonzalez-Huici et al., 2014).

Another key issue in the function of DDT mechanisms is when and where they operate (i.e., coupled to replication forks or post-replicatively). There is convincing evidence that TLS and damage avoidance function behind replication forks, probably promoting gap filling (Branzei et al., 2008; Daigaku et al., 2010; Huang et al., 2013; Karras and Jentsch, 2010; Lopes et al., 2006). However, the Rad5-dependent, error-free branch may facilitate the restart of forks stalled by DNA damage, at least near replication origins (Minca and Kowalski, 2010). Also in favor of a possible fork-associated process, Rad5 and HLTF have been shown to promote fork regression in vitro (Blastyák et al., 2007, 2010), although it is unknown whether this also occurs in vivo.

Here, we analyze the contribution of the two branches of the *RAD6/RAD18* pathway to the tolerance to replication-blocking DNA lesions, using budding yeast and the model DNA-damaging agent MMS. We show that the Rad5-dependent DNA damage-avoidance subpathway performs the principal role in this cellular response and that Rad5 has a key function at forks, allowing replication through damaged DNA.

RESULTS

Tolerance to MMS-Induced DNA Lesions during S Phase Is Carried Out Predominantly by the Rad5-Dependent Damage-Avoidance Pathway

To assess the relative contributions of the two branches of the *RAD6/RAD18* pathway to chromosome replication over DNA lesions, we limited DNA damage to a single S phase and studied the consequences of a lack of TLS polymerases or Rad5. Control and mutant cells were synchronized in G1 and released into medium with or without 0.033% MMS. In the absence of MMS, all cells completed S phase by 60 min and continued cycling, whereas they progressed slowly through S phase in medium with MMS due to the DNA lesions (Paulovich and Hartwell, 1995; Tercero and Diffley, 2001; Figure 1A). Flow-cytometry analysis indicated no apparent differences between wild-type (WT) and *tls*Δ (*rev3*Δ*rad30*Δ*rev1*Δ) cells in S-phase progression when the cells were treated with MMS. However, *rad5*Δ cells showed increased defects and, unlike WT or *tls*Δ cells, most of these cells did not reach a 2C DNA content (Figure 1A). Lack of TLS polymerases or Rad5 did not cause replication perturbations per se, as the S-phase checkpoint was not activated if cells were not exposed to DNA damage. After MMS exposure, the checkpoint was activated normally in all strains, as Rad53 was phosphorylated and acquired kinase activity (Figure 1A).

We repeated the above experiment with a much lower dose of MMS (0.0033%) that neither delayed cell-cycle progression nor activated Rad53 in WT cells (Figure 1B). *tls*Δ cells were also unaffected by exposure to 0.0033% MMS, as they cycled normally and did not activate Rad53 (Figure 1B). However, the same treatment impeded the progression of *rad5*Δ cells through the cell cycle, and cells remained blocked with a 2C DNA content as large budded cells with undivided chromatin (Figures 1B and S1). Furthermore, in contrast to WT and *tls*Δ cells, Rad53 was activated in *rad5*Δ cells (Figure 1B). Although *rad5*Δ cells reached a 2C DNA content, checkpoint activation was due to problems during replication, since when the cells were blocked in G2/M and then treated with 0.0033% MMS, neither Rad53 phosphorylation nor Rad53 kinase activity was triggered (Figure S1). These results identify a crucial function for Rad5 in the response to MMS-induced DNA damage during S phase.

We next examined cell viability upon treatment with several concentrations of MMS during S phase. Whereas WT cells showed high viability and *tls*Δ cells were only moderately sensitive at the highest MMS doses, *rad5*Δ cells exhibited a dramatic drop in viability after MMS treatment and were sensitive to the lowest MMS dose (Figure 1C). *rad5*Δ showed a slightly less marked loss of viability than *rad18*Δ, whereas *tls*Δ*rad5*Δ and *rad18*Δ cells showed a similar viability (Figure 1C), suggesting that the extreme sensitivity of Rad18-deficient cells to MMS is due to the lack of Rad5 and TLS functions. Thus, both branches of the *RAD6/RAD18* pathway are important for dealing with MMS-induced DNA lesions during S phase. However, it is clear that the DNA damage-avoidance branch, mediated by Rad5, has the major role in this response and TLS makes only a minor contribution.

Rad5 Is Required for the Progression of Replication Forks through Damaged DNA

The above data indicate a central role for Rad5 in tolerance to MMS-induced DNA damage during S phase, pointing to an important function of this protein in replication of damaged chromosomes. However, it was previously proposed that *rad5*Δ cells could replicate through MMS-damaged DNA without delay (Karras and Jentsch, 2010). To analyze chromosome replication under these DNA-damaging conditions, we used dense isotope transfer, which allows one to study ongoing DNA synthesis at a specific replicon by analyzing the movement of replication forks (Tercero et al., 2000).

WT, *tls*Δ, and *rad5*Δ cells were grown in medium with "heavy" isotopes, synchronized in G1, and released into medium with "light" isotopes, either with or without MMS. The replication of six DNA fragments was followed in a replicon of chromosome VI (Tercero and Diffley, 2001) from the *ARS607* origin to the end of the chromosome (Figure 2). All DNA fragments were in the "heavy-heavy" (HH; unreplicated DNA) peak in G1 cells (top row). In all cases, DNA fragments shifted to the "heavy-light" (HL; replicated DNA) peak by 60 min in medium without MMS (bottom row), indicating that they had been replicated. In WT cells, fragment 1 containing *ARS607* shifted to the HL peak by 30 min following release into medium with MMS, and some HL DNA was also apparent in fragment 2 (Figure 2A). DNA replication advanced rightward: fragment 3 shifted to the HL position by 60 min and replication of the remaining fragments proceeded progressively (replication is quantified in Figure 2D). Thus, as described previously (Tercero and Diffley, 2001; Vázquez et al., 2008), the forks progressed slowly through damaged DNA but were able to replicate the entire replicon. Fork progression in the presence of MMS in *tls*Δ cells was similar to that in WT cells: fragments 1 and 2 shifted to the HL peak by 30 min; forks progressed slowly from left to right, and by 240 min the replicon was mostly replicated (Figures 2B and 2D). Thus, TLS polymerases are not required for fork progression through MMS-damaged DNA.

In the *rad5*Δ mutant, the DNA fragment 1 shifted to the HL peak by 30 min in medium containing MMS (Figure 2C), showing that *ARS607* fired as in WT cells. Forks moved slowly and DNA replication advanced rightward, as indicated by the progressive shifting of the restriction fragments to the HL peak. However, there were notable differences between *rad5*Δ and WT cells. Thus, the percentage of replicated (HL) DNA of fragments 2–6 at 120 min was markedly reduced in the *rad5*Δ mutant in comparison with WT cells (Figures 2C and 2D). At 240 min, when the replicon was mostly replicated in WT cells, a considerable amount of DNA remained unreplicated (HH peak) in fragments 2–6 in *rad5*Δ cells. Indeed, only about 25% of the forks had reached the end of the replicon at the latest time point measured.

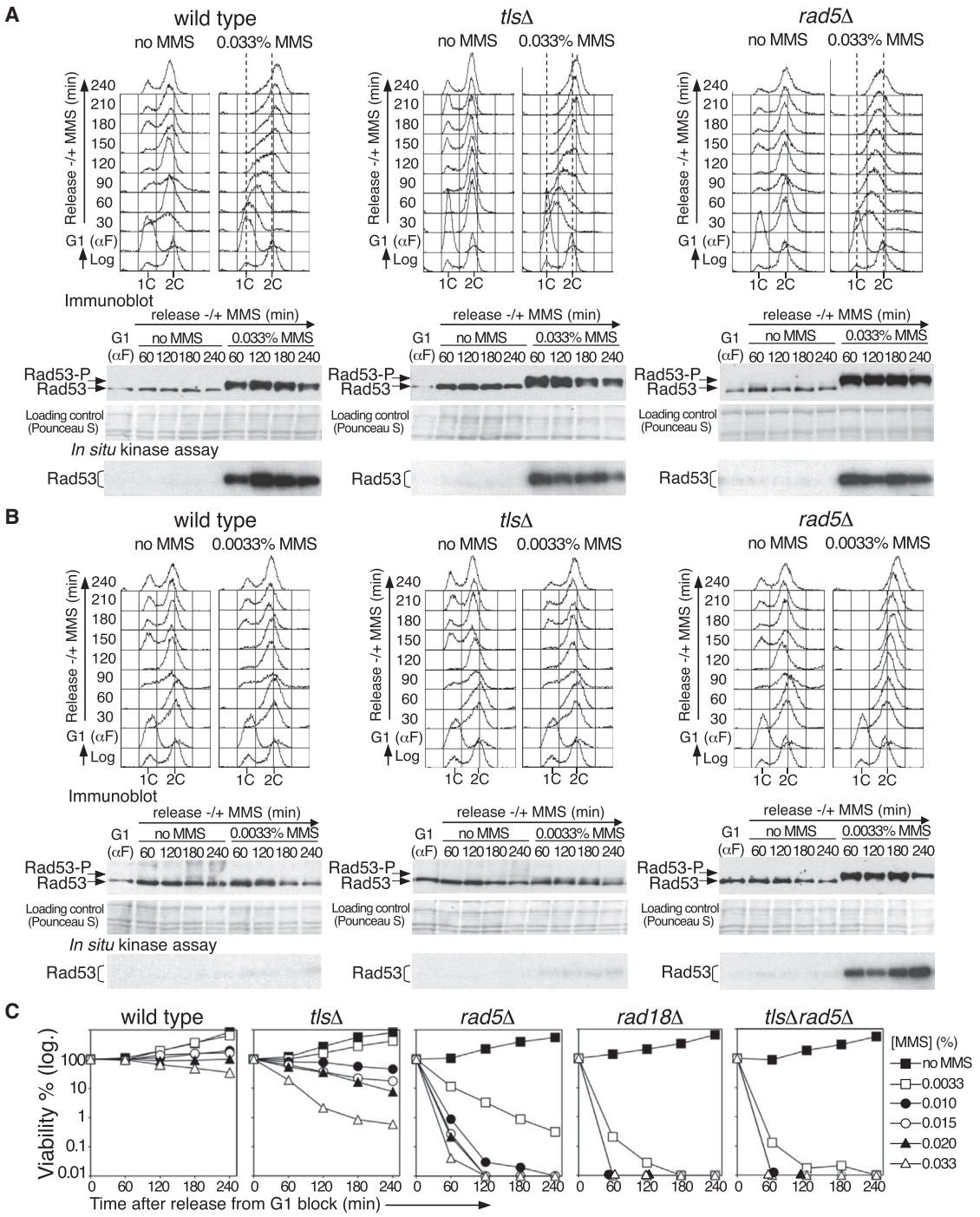

Figure 1. Rad5 Has a Major Role in Tolerance to MMS-Induced DNA Lesions during S Phase

(A and B) WT (YMO13 strain), *tls*Δ (YMO27), and *rad5*Δ (YMO18) cells were blocked in G1 using α-factor and released into medium ± 0.033% MMS (A) or ± 0.0033% MMS (B). Upper panel: DNA content was determined by flow cytometry to follow cell-cycle progression. Bottom panel: immunoblot and in situ autophosphorylation analysis of Rad53.

(C) G1-blocked cells were released into S phase in the presence of different MMS concentrations. Cell viability was estimated at the indicated time points. *rad18*Δ (YJT116 strain); *tls*Δ*rad5*Δ (YMO28).

See also Figure S1.

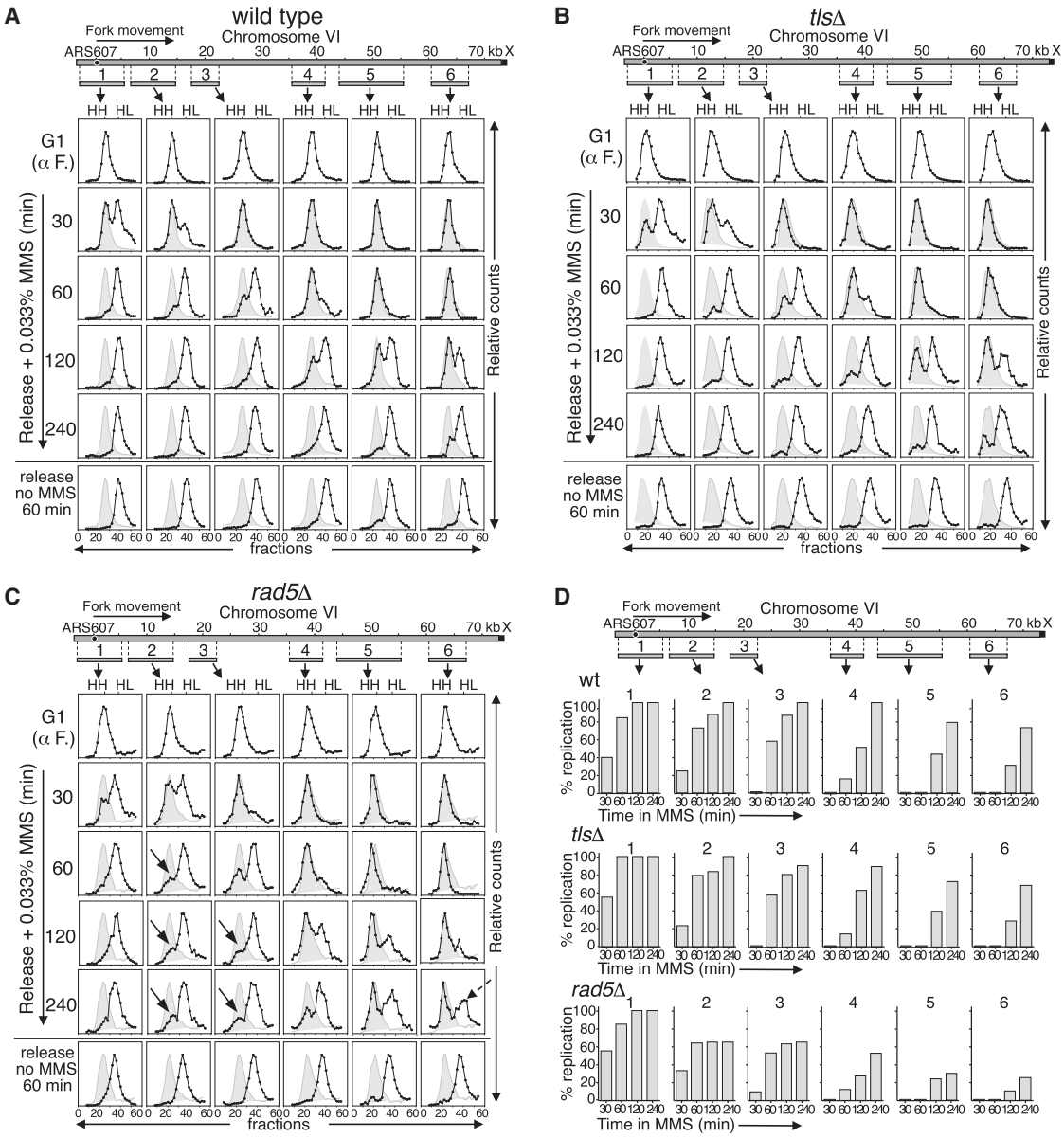

Figure 2. Rad5 Is Required for DNA Replication Fork Progression through Damaged DNA

(A–C) The progression of DNA replication forks was analyzed by density transfer. (A) WT (YMO13 strain), (B) *tls*Δ (YMO27), and (C) *rad5*Δ (YMO18) cells were blocked in G1 with α-factor in medium with heavy isotopes and then released into medium with light isotopes ± MMS (0.033%). Fork progression was followed in a replicon of chromosome VI using probes that recognize the *Cla*I/*Sal*I fragments 1–6 (Tercero and Diffley, 2001). The relative amounts of radioactivity in the hybridized DNA are plotted against the gradient fraction number. Unreplicated (HH) and fully replicated (HL) peaks are indicated. The position of the initial HH peak is shown for comparison (gray area). Solid arrows indicate persistent unreplicated DNA in *rad5*Δ cells. The dashed arrow indicates the small amount of replicated DNA in *rad5*Δ cells at the end of the replicon at the latest time point (fragment 6, 240 min).

(D) Quantification of DNA replication in the presence of MMS for every DNA fragment and time point.

See also Figures S1 and S3.

Remarkably, the percentage of replicated DNA (~65%) in fragments 2 and 3 did not further increase after 60 min, indicating that a significant fraction of forks stalled or collapsed before passing them. The average size of a replicon in budding yeast is 40 kb and thus forks normally travel ~20 kb. We estimated that about one-third of the forks terminated before 20 kb from the *ARS607* origin in *rad5*Δ cells after 240 min of MMS treatment. Therefore, these results show that Rad5 is necessary for the extensive progression of replication forks through MMS-damaged DNA. Moreover, these data could explain why *rad5*Δ cells lose viability when treated with MMS during S phase (Figure 1C).

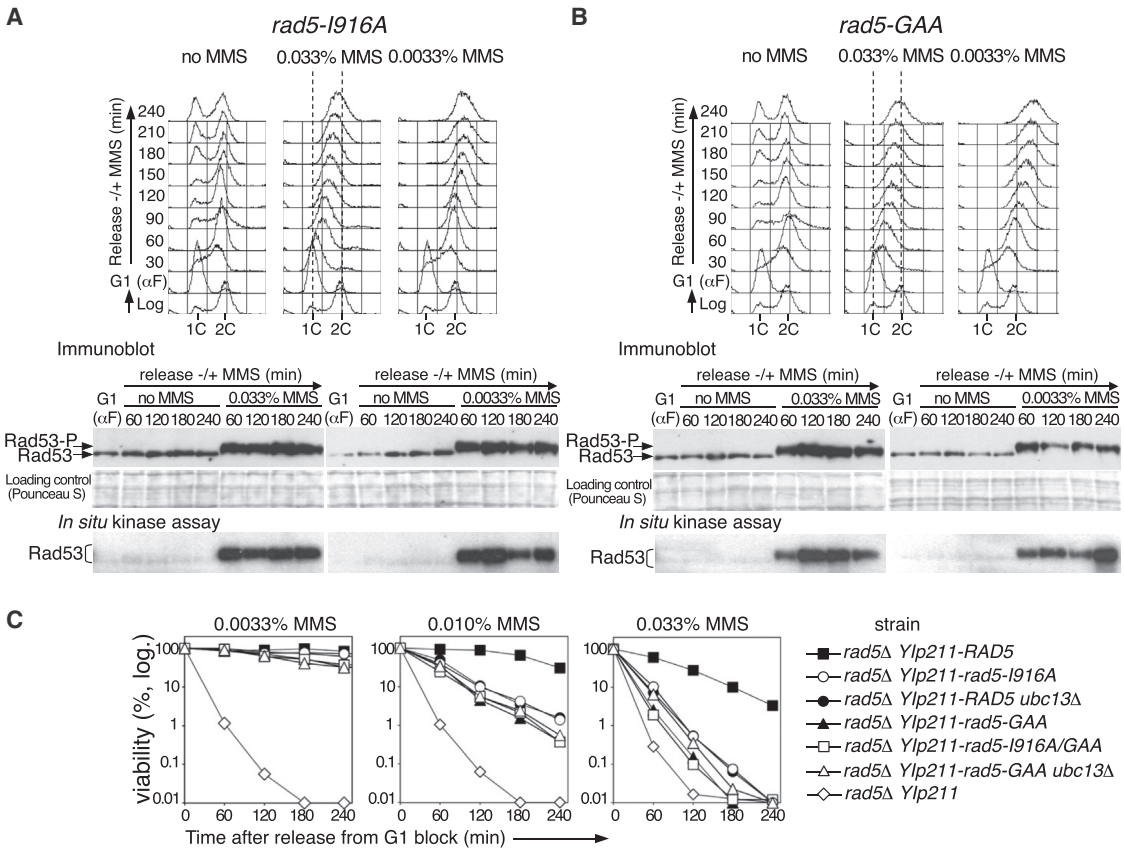

Figure 3. Rad5-Ubiquitin Ligase and ATPase/Helicase Activities Are Required for the DNA Damage Response during S Phase

(A and B) (A) *rad5-I916A* cells (YMO60 strain) and (B) *rad5-GAA* cells (YMO57 strain) were blocked in G1 using α-factor and released into medium ± MMS (0.033% or 0.0033%). Upper panel: cell-cycle progression was followed by flow cytometry. Bottom panel: immunoblot and in situ autophosphorylation analysis of Rad53. (C) G1-blocked cells were released into S phase in medium containing different concentrations of MMS. Cell viability was estimated at the indicated time points. The strains (all isogenic) were *RAD5*$^{+}$ control (YMO56 strain), *rad5-I916A* (YMO60), *ubc13*Δ (YMO69), *rad5-GAA* (YMO57), *rad5-I916A/GAA* (YMO63), *rad5-GAAubc13*Δ (YMO71), and *rad5*Δ control (YMO55).

See also Figures S2 and S3.

The Ubiquitin-Ligase and ATPase/Helicase Activities of Rad5 Are Required for the Response to MMS-Induced DNA Damage during S Phase

To determine the contribution of the known activities of Rad5 to the response to MMS-induced DNA lesions, we generated strains harboring *RAD5* mutations that eliminate either its ubiquitin-ligase activity (*rad5-I916A*) (Ulrich, 2003) or ATPase activity (*rad5-K538A/T539A*, or *rad5-GAA*) (Chen et al., 2005; Figure S2), and then we used the same approach described above.

rad5-I916A and *rad5-GAA* cells cycled normally, but in comparison with WT and *tls*Δ cells, S-phase progression was delayed in the presence of 0.033% MMS (Figures 1A, 3A, and 3B). When exposed to 0.0033% MMS, a dose that does not affect WT or *tls*Δ cells (Figure 1B), the *rad5-I916A* and *rad5-GAA* mutants could not progress through the cell cycle and, like the *rad5*Δ cells (Figure 1B), remained blocked with a 2C DNA content (Figures 3A and 3B). Moreover, Rad53 was phosphorylated and acquired kinase activity, indicating checkpoint activation at this low MMS dose (Figures 3A and 3B), mirroring the results with *rad5*Δ (Figure 1B). Consistently, a *ubc13*Δ strain, in which PCNA cannot be polyubiquitylated due to defective E2-ubiquitin conjugating activity, behaved as *rad5-I916A* (Figure S2). Therefore, the ubiquitin-ligase and ATPase activities of Rad5 are important for its functional response to MMS. Strengthening this conclusion, density transfer experiments showed that *rad5-I916A, rad5-GAA*, and *ubc13*Δ mutants were defective in fork progression through MMS-damaged DNA (Figure S3).

In support of our conclusion that ubiquitin-ligase and ATPase activities are required for tolerance to MMS-induced DNA lesions, both *rad5-I916A* and *rad5-GAA* mutants lost viability significantly in comparison with an isogenic *RAD5*$^{+}$ control strain when treated with 0.01% or 0.033% MMS during S phase (Figure 3C). Also, the viability of an isogenic *ubc13*Δ strain was similar to that of *rad5-I916A*. The decrease in viability of these *rad5* mutants was not as extreme as that found for *rad5*Δ cells; thus, we constructed a double *rad5-I916A/GAA* mutant to assess whether the effects of lacking both activities were synergistic. As shown in Figure 3C, *rad5-I916A/GAA* cells did not present increased sensitivity to MMS with respect to the most sensitive individual mutant, *rad5-GAA*. In agreement with the above data, the sensitivity of the *rad5-GAAubc13*Δ strain was similar to that of *rad5-I916A/GAA* cells. Therefore, at least in

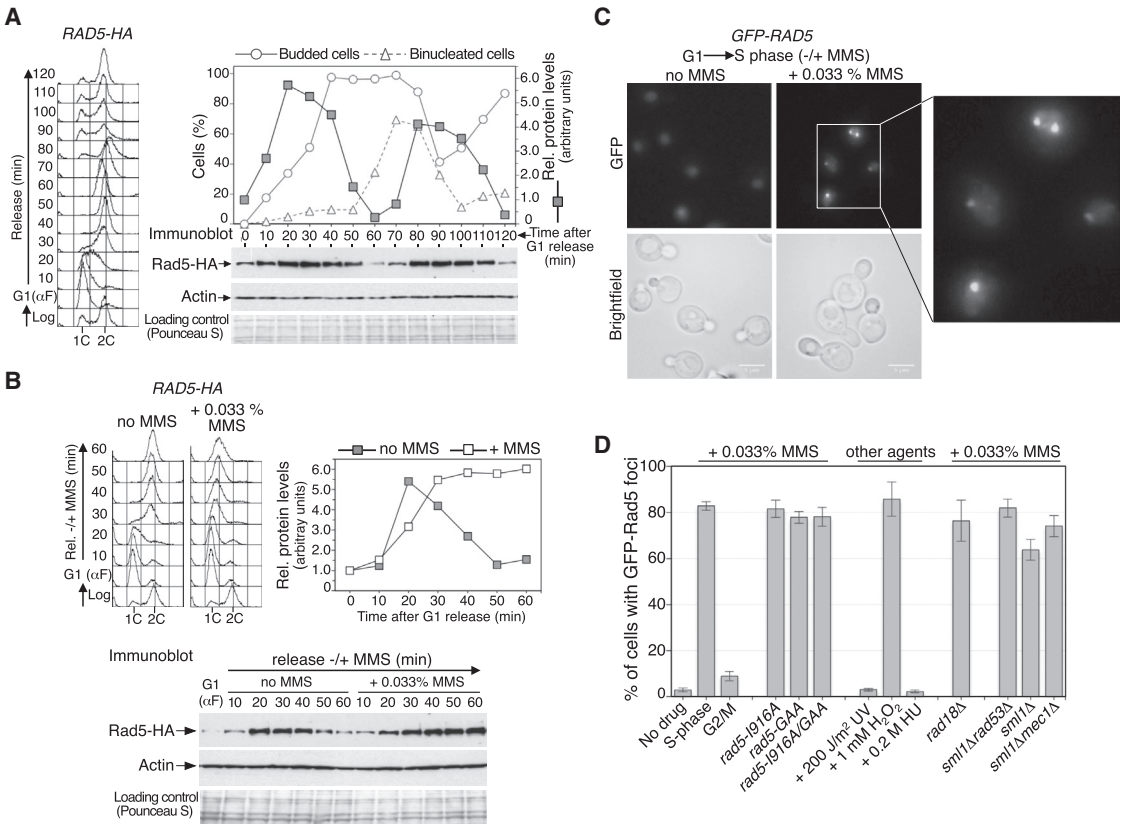

Figure 4. Rad5 Regulation

(A) *RAD5-HA* cells (YMO52 strain) were synchronized in G1 and then released into fresh medium. Cell-cycle progression was analyzed by flow cytometry (left). The percentage of budded and binucleated cells was estimated throughout the experiment (right). Rad5 immunoblot analysis is shown below. The relative protein levels are depicted for every time point.

(B) G1-synchronized *RAD5-HA* cells (YMO52 strain) were released into medium ± MMS (0.033%). Cell-cycle progression was analyzed by flow cytometry (upper panel, left). Immunoblot analysis of Rad5 (bottom panel). The relative protein levels are depicted (upper panel, right).

(C) *GFP-RAD5* cells (YMO36 strain) were synchronized in G1 using α-factor, released into S phase in medium either without MMS (for 30 min) or with 0.033% MMS (for 60 min), and analyzed by fluorescence microscopy.

(D) Percentage of cells with GFP-Rad5 foci under several conditions and in different mutants. For MMS treatment, cells were blocked in G1, released into S phase and exposed to 0.033% MMS for 60 min, or treated for 60 min with 0.033% once they were blocked in G2/M. UV-treated cells were analyzed 30 min (in the dark) after 200 J/m^2 UV exposure in G1 and release into S phase. Cells were treated with 1 mM H_2O_2 for 30 min after release into S phase from a G1 block. Cells were treated with 0.2 M HU for 120 min after release from a G1 block. The histograms represent the mean ± SD from three independent experiments.

See also Figure S4.

terms of tolerance to MMS, *rad5-I916A* and *rad5-GAA* mutants are epistatic, suggesting that the Rad5 ubiquitin-ligase and ATPase/helicase actions work sequentially and not independently. The fact that *rad5-I916A/GAA* cells are less sensitive to MMS than the isogenic *rad5*Δ control (Figure 3C) could be explained by additional Rad5 functions in DDT. In this regard, Rad5 controls some TLS events (Coulon et al., 2010; Gangavarapu et al., 2006; Pagès et al., 2008), and its human homologs, HLTF and SHPRH, promote the recruitment of the most appropriate TLS polymerase to the sites of damage (Lin et al., 2011).

Rad5 Is a Periodic Protein that Peaks in S Phase and, in Response to DNA Damage, Forms Subnuclear Foci

To study the potential regulation of Rad5, we first analyzed its expression throughout the cell cycle. *RAD5-HA* cells were synchronized in G1, released, and allowed to cycle. Rad5 expression oscillated significantly along the cell cycle (Figure 4A). Thus, Rad5 reached maximum levels at 20–30 min after G1 release, indicating a peak of expression in early-mid S phase. Thereafter, protein levels decreased and reached a minimum at the end of S phase or mitosis (50–70 min after G1), rising again during the S phase of the second cell cycle (~90 min) (Figure 4A). This result strongly suggests that Rad5 acts predominantly during S phase, and is consistent with its role in chromosomal replication in the face of DNA damage. Similar results were obtained with Rad5-GFP, eliminating the possibility that the observed oscillations were due to the epitope tag used (Figure S4).

To study whether Rad5 was regulated in response to DNA damage, we released G1-blocked cells into S phase in medium with and without MMS (Figure 4B). In drug-free medium, Rad5 oscillated as before. In medium containing MMS, Rad5 showed maximum levels that were similar to those reached in the

absence of DNA damage. Further, these levels were maintained during the experiment due to the prolonged S phase. Thus, MMS treatment during S phase does not significantly influence Rad5 levels. Therefore, Rad5 expression is independent of exogenous DNA damage.

We next analyzed Rad5 in vivo by fluorescence microscopy. In untreated cells, Rad5 appeared spread in the nucleus, but it accumulated and formed subnuclear foci after exposure to 0.033% MMS during S phase (Figure 4C). These foci were visible in approximately 80% of the cells (quantification is shown in Figure 4D) and usually appeared as one or two discrete dots per cell (Figure 4C). Therefore, Rad5 relocalized within the nucleus in response to MMS-induced DNA damage, even though its levels did not show significant changes after MMS exposure (Figure 4B). Rad5-foci formation was clearly seen in S phase, but was not detected in G2/M-blocked cells treated with MMS (Figures S4 and 4D), supporting a function for Rad5 during S phase. The ubiquitin-ligase and ATPase/helicase activities of Rad5 were not required for formation of these foci (Figures S4 and 4D), signifying that this response is independent of its catalytic activity. Rad5 relocalization also occurred after treatment with other DNA-damaging agents, such as H_2O_2 (Figures S4 and 4D). However, no foci were detected after UV light exposure (Figures S4 and 4D), presumably because TLS is more important than damage avoidance for tolerance to acute UV treatment (Daigaku et al., 2010). In a recent high-throughput screening, Tkach et al. (2012) identified Rad5 as one of the proteins that showed localization changes following drug-induced replication stress. Our results agree with and extend their data regarding Rad5 relocalization upon exposure of asynchronously growing cells to 0.03% MMS, but differ from their data suggesting that Rad5 foci formed after treatment with 0.2 M hydroxyurea (HU). In our strains, we could not detect Rad5 foci when cells were treated with 0.2 M HU after release from a G1 block (Figures S4 and 4D). Analogously to MMS, 0.2 M HU causes fork stalling (Tercero et al., 2000), but unlike MMS, it does not necessarily invoke DNA damage. Therefore, only fork blocks caused by some DNA lesions lead to Rad5 foci formation. Interestingly, the formation of DNA-damage-induced Rad5 foci is Rad18 independent, as they were detected in MMS-treated *rad18*Δ cells (Figures S4 and 4D). Also, Rad5 foci formation does not require the activation of the S phase checkpoint triggered by MMS, as they also appeared in the checkpoint-deficient strains *mec1*Δ and *rad53*Δ after exposure to this drug (Figures S4 and 4D).

DISCUSSION

We show in this work that the DNA damage-avoidance branch of the *RAD6*/*RAD18* pathway, mediated by Rad5, has the principal role in tolerance to MMS-induced DNA lesions during chromosome replication. This choice ensures an error-free process and minimizes the risk of mutagenesis. Interestingly, cells respond differently to another commonly used DNA-damaging treatment, acute UV exposure, because TLS is the main mechanism of lesion bypass in this case (Daigaku et al., 2010). Similarly, human cells also preferentially use TLS in response to environmental agents (Izhar et al., 2013). These data demonstrate that cells employ different efficient strategies to tolerate diverse DNA insults.

Our results show that the Rad5-mediated cellular response allows chromosome replication under conditions of DNA damage. Both the ubiquitin-ligase and ATPase/helicase activities of Rad5 are required for this process. We show that Rad5 is required for fork progression through MMS-damaged DNA, indicating a direct role for this protein at forks. However, DDT mechanisms are operational after the bulk of genome replication has been completed (Daigaku et al., 2010; Karras and Jentsch, 2010), which together with other findings indicates that they could function postreplicatively, behind replication forks (Branzei et al., 2008; Daigaku et al., 2010; Huang et al., 2013; Karras and Jentsch, 2010; Lopes et al., 2006). Regardless of whether this pathway operates at forks or postreplicatively, it is likely that Rad5 acts through a recombinational mechanism in both cases, originating X-shaped DNA structures that involve sister chromatid junctions (Branzei et al., 2008; Minca and Kowalski, 2010). Nevertheless, the fact that Rad5 can work at forks leaves open the possibility that it can also promote fork regression (Blastyák et al., 2007). Taking all of these considerations into account, we propose that the Rad5-dependent, error-free branch of the *RAD6*/*RAD18* pathway operates normally during S phase and that its action can occur both directly at forks and in the rear of continuing replication, which might depend upon the types of lesions or the particular sites of damage. The mode of action of Rad5 reflects a robust system of DNA damage avoidance that can function even after bulk DNA synthesis.

Consistent with its role in promoting fork progression through damaged DNA, we found that Rad5 has a peak of expression during S phase. This regulation is different from that of other DDT proteins, such as Rev1, whose levels peak in G2/M (Waters and Walker, 2006), supporting a TLS function after bulk DNA replication. We also show that in response to MMS, Rad5 accumulates and forms subnuclear foci in S phase. This relocalization is Rad18 independent, which would be in agreement with the independent association of Rad18 and Rad5 to chromatin despite their colocalization (Ulrich and Jentsch, 2000). In addition, we found that Rad5 foci are also formed in the absence of the S phase checkpoint, which indicates independent signaling pathways. Together, our results extend our understanding of how the Rad5-dependent pathway is regulated in response to DNA lesions. As a consequence of some types of DNA damage, Rad18 is recruited to chromatin, Rad5 is independently relocalized and forms subnuclear foci in S phase, and its E2 ubiquitin-conjugating counterparts Ubc13 and Mms2 relocalize from the cytoplasm to the nucleus (Ulrich and Jentsch, 2000), with all of these processes occurring in parallel but independently of checkpoint activation. It is possible that accumulation of Rad5 facilitates its interaction with Rad18 and Ubc13/Mms2, as well as its access to DNA lesions, thereby contributing to the damage-avoidance process.

Rad5 is critical for genome integrity. It sidesteps mutagenesis, which is directly related to cancer development. Indeed, the *RAD5* human orthologs *HLTF* and *SHPRH* are inactivated in some cancer cells (Debauve et al., 2008; Sood et al., 2003). An extrapolation of the results from this work would imply that some tumor cells could be extremely sensitive to drugs that

interfere with DNA replication due to defects in the error-free branch of the *RAD6/RAD18* pathway. This scenario could be explored to improve chemotherapy strategies.

EXPERIMENTAL PROCEDURES

Strains and Media

The yeast strains used in this work are listed in Table S1. Yeasts were routinely grown in YP medium with 2% glucose.

Cell-Cycle Blocks, Flow Cytometry, Cell Viability, and Microscopy

α-Factor (5–10 μg/ml) was used for G1 synchronization. Flow cytometry was performed as previously described (Vázquez et al., 2008). Cell viability was determined by plating cells in triplicate and counting colony-forming units after 3 days of incubation at 30°C. The numerical data are the average of comparable experiments. For fluorescence microscopy, cells were grown in minimal medium supplemented with yeast synthetic dropout. Live cells were analyzed using an Axiovert 200 fluorescence microscope (Zeiss). The percentage of cells containing foci was estimated after analyzing three independent experiments, and at least 300 cells were counted in each experiment.

Immunoblotting and In Situ Kinase Assays

Protein extracts were prepared from trichloroacetic acid-treated cells (Vázquez et al., 2008). Hemagglutinin-tagged proteins were detected with the 12CA5 antibody (CBMSO) and GFP-tagged proteins were detected with an anti-GFP antibody (Roche). Anti-Actin antibody was obtained from MP Biomedicals. The secondary antibody was horseradish peroxidase (HRP)-coupled anti-mouse (Vector Labs). Rad53 was detected with the JDI48 antibody (J. Diffley, Cancer Research UK) using HRP-coupled Protein A (Invitrogen) as a secondary antibody. Quantification of protein bands was carried out using a GS-800 densitometer (BioRad) and density was normalized to actin. The Rad53 in situ kinase assay was performed as described previously (Vázquez et al., 2008).

Dense Isotope Transfer

Density transfer assays were performed as previously described (Tercero et al., 2000). The extent of replication was calculated as follows: % replication = 100(0.5 HL/(HH+0.5 HL)).

SUPPLEMENTAL INFORMATION

Supplemental Information includes four figures and one table and can be found with this article online at http://dx.doi.org/10.1016/j.celrep.2014.09.005.

ACKNOWLEDGMENTS

We thank C. Gutiérrez for a critical reading of the manuscript, H. Ulrich for the plasmids containing the *rad5*-point mutants, and J. Diffley for the anti-Rad53 antibody. This work was supported by the Spanish Ministry of Economy and Competitiveness (MINECO; grants BFU2010-16989, BFU2013-43766, and Consolider Ingenio CSD2007-00015). M.A.O.-B. and A.J.-M. are the recipients of predoctoral fellowships from MINECO. M.G.-F. is the recipient of a predoctoral fellowship from UAM. The CBMSO receives an institutional grant from Fundación Ramón Areces.

Received: May 12, 2014
Revised: August 13, 2014
Accepted: August 29, 2014
Published: October 9, 2014

REFERENCES

Blastyák, A., Pintér, L., Unk, I., Prakash, L., Prakash, S., and Haracska, L. (2007). Yeast Rad5 protein required for postreplication repair has a DNA helicase activity specific for replication fork regression. Mol. Cell *28*, 167–175.

Blastyák, A., Hajdú, I., Unk, I., and Haracska, L. (2010). Role of double-stranded DNA translocase activity of human HLTF in replication of damaged DNA. Mol. Cell. Biol. *30*, 684–693.

Branzei, D. (2011). Ubiquitin family modifications and template switching. FEBS Lett. *585*, 2810–2817.

Branzei, D., Vanoli, F., and Foiani, M. (2008). SUMOylation regulates Rad18-mediated template switch. Nature *456*, 915–920.

Chang, D.J., and Cimprich, K.A. (2009). DNA damage tolerance: when it's OK to make mistakes. Nat. Chem. Biol. *5*, 82–90.

Chen, S., Davies, A.A., Sagan, D., and Ulrich, H.D. (2005). The RING finger ATPase Rad5p of *Saccharomyces cerevisiae* contributes to DNA double-strand break repair in a ubiquitin-independent manner. Nucleic Acids Res. *33*, 5878–5886.

Coulon, S., Ramasubramanyan, S., Alies, C., Philippin, G., Lehmann, A., and Fuchs, R.P. (2010). $Rad8^{Rad5}$/Mms2-Ubc13 ubiquitin ligase complex controls translesion synthesis in fission yeast. EMBO J. *29*, 2048–2058.

Daigaku, Y., Davies, A.A., and Ulrich, H.D. (2010). Ubiquitin-dependent DNA damage bypass is separable from genome replication. Nature *465*, 951–955.

Debauve, G., Capouillez, A., Belayew, A., and Saussez, S. (2008). The helicase-like transcription factor and its implication in cancer progression. Cell. Mol. Life Sci. *65*, 591–604.

Gangavarapu, V., Haracska, L., Unk, I., Johnson, R.E., Prakash, S., and Prakash, L. (2006). Mms2-Ubc13-dependent and -independent roles of Rad5 ubiquitin ligase in postreplication repair and translesion DNA synthesis in *Saccharomyces cerevisiae*. Mol. Cell. Biol. *26*, 7783–7790.

Gonzalez-Huici, V., Szakal, B., Urulangodi, M., Psakhye, I., Castellucci, F., Menolfi, D., Rajakumara, E., Fumasoni, M., Bermejo, R., Jentsch, S., and Branzei, D. (2014). DNA bending facilitates the error-free DNA damage tolerance pathway and upholds genome integrity. EMBO J. *33*, 327–340.

Hishida, T., Kubota, Y., Carr, A.M., and Iwasaki, H. (2009). RAD6-RAD18-RAD5-pathway-dependent tolerance to chronic low-dose ultraviolet light. Nature *457*, 612–615.

Huang, D., Piening, B.D., and Paulovich, A.G. (2013). The preference for error-free or error-prone postreplication repair in *Saccharomyces cerevisiae* exposed to low-dose methyl methanesulfonate is cell cycle dependent. Mol. Cell. Biol. *33*, 1515–1527.

Izhar, L., Ziv, O., Cohen, I.S., Geacintov, N.E., and Livneh, Z. (2013). Genomic assay reveals tolerance of DNA damage by both translesion DNA synthesis and homology-dependent repair in mammalian cells. Proc. Natl. Acad. Sci. USA *110*, E1462–E1469.

Karras, G.I., and Jentsch, S. (2010). The *RAD6* DNA damage tolerance pathway operates uncoupled from the replication fork and is functional beyond S phase. Cell *141*, 255–267.

Lin, J.R., Zeman, M.K., Chen, J.Y., Yee, M.C., and Cimprich, K.A. (2011). SHPRH and HLTF act in a damage-specific manner to coordinate different forms of postreplication repair and prevent mutagenesis. Mol. Cell *42*, 237–249.

Lopes, M., Foiani, M., and Sogo, J.M. (2006). Multiple mechanisms control chromosome integrity after replication fork uncoupling and restart at irreparable UV lesions. Mol. Cell *21*, 15–27.

Minca, E.C., and Kowalski, D. (2010). Multiple Rad5 activities mediate sister chromatid recombination to bypass DNA damage at stalled replication forks. Mol. Cell *38*, 649–661.

Pagès, V., Bresson, A., Acharya, N., Prakash, S., Fuchs, R.P., and Prakash, L. (2008). Requirement of Rad5 for DNA polymerase zeta-dependent translesion synthesis in *Saccharomyces cerevisiae*. Genetics *180*, 73–82.

Paulovich, A.G., and Hartwell, L.H. (1995). A checkpoint regulates the rate of progression through S phase in *S. cerevisiae* in response to DNA damage. Cell *82*, 841–847.

Sale, J.E. (2013). Translesion DNA synthesis and mutagenesis in eukaryotes. Cold Spring Harb. Perspect. Biol. *5*, a012708.

Saugar, I., Ortiz-Bazan, M.A., and Tercero, J.A. (2014). Tolerating DNA damage during eukaryotic chromosome replication. Exp. Cell. Res., Published online July 17 http://dx.doi.org/10.1016/j.yexcr.2014.07.009.

Sood, R., Makalowska, I., Galdzicki, M., Hu, P., Eddings, E., Robbins, C.M., Moses, T., Namkoong, J., Chen, S., and Trent, J.M. (2003). Cloning and characterization of a novel gene, SHPRH, encoding a conserved putative protein with SNF2/helicase and PHD-finger domains from the 6q24 region. Genomics *82*, 153–161.

Tercero, J.A., and Diffley, J.F. (2001). Regulation of DNA replication fork progression through damaged DNA by the Mec1/Rad53 checkpoint. Nature *412*, 553–557.

Tercero, J.A., Labib, K., and Diffley, J.F. (2000). DNA synthesis at individual replication forks requires the essential initiation factor Cdc45p. EMBO J. *19*, 2082–2093.

Tkach, J.M., Yimit, A., Lee, A.Y., Riffle, M., Costanzo, M., Jaschob, D., Hendry, J.A., Ou, J., Moffat, J., Boone, C., et al. (2012). Dissecting DNA damage response pathways by analysing protein localization and abundance changes during DNA replication stress. Nat. Cell Biol. *14*, 966–976.

Ulrich, H.D. (2003). Protein-protein interactions within an E2-RING finger complex. Implications for ubiquitin-dependent DNA damage repair. J. Biol. Chem. *278*, 7051–7058.

Ulrich, H.D. (2011). Timing and spacing of ubiquitin-dependent DNA damage bypass. FEBS Lett. *585*, 2861–2867.

Ulrich, H.D., and Jentsch, S. (2000). Two RING finger proteins mediate cooperation between ubiquitin-conjugating enzymes in DNA repair. EMBO J. *19*, 3388–3397.

Unk, I., Hajdú, I., Blastyák, A., and Haracska, L. (2010). Role of yeast Rad5 and its human orthologs, HLTF and SHPRH in DNA damage tolerance. DNA Repair (Amst.) *9*, 257–267.

Vázquez, M.V., Rojas, V., and Tercero, J.A. (2008). Multiple pathways cooperate to facilitate DNA replication fork progression through alkylated DNA. DNA Repair (Amst.) *7*, 1693–1704.

Waters, L.S., and Walker, G.C. (2006). The critical mutagenic translesion DNA polymerase Rev1 is highly expressed during G(2)/M phase rather than S phase. Proc. Natl. Acad. Sci. USA *103*, 8971–8976.